New Cadmium(II) and Iron(II) Coordination Frameworks Incorporating a Di(4-pyridyl)isoindoline Ligand

Yanyan Mulyana,[a] Cameron J. Kepert,*[a] Leonard F. Lindoy,*[a] and John C. McMurtrie[a,b]

Keywords: Cadmium / Iron / Molecular framework

The metal-directed assembly of molecular frameworks incorporating the ditopic heterocyclic ligand 1-(4-pyridyl)imino-2-(4-pyridyl)isoindoline (**L**) associated with nonlinear coordination vectors, is presented. Two infinite metallo-arrays of empirical formula $[Cd\mathbf{L}(NO_3)_2(EtOH)]_n\cdot(1.4\,H_2O)_n$ and $[Fe\mathbf{L}_2(NCS)_2]_n\cdot\{(2\,CHClCCl_2)\cdot(1.4\,MeOH)\cdot(2.9\,H_2O)\}_n$ have been characterised. The X-ray structures of both arrays are reported. The cadmium(II) framework consists of co-aligned 1D coordinate polymer chains while the iron(II) framework consists of rhombic grids with 2D polymeric connectivity.

Introduction

The assembly of metal-organic frameworks is an area of much current interest[1a–1k,2] since the porous structures characteristic of such materials frequently show selective guest molecule uptake (or exchange) from vapours,[3a–3e] solution[3a–3e] and gases[4a,4b] as well as promoting heterogeneous catalysis in a number of cases.[5] While a wide range of organic components has now been incorporated in such frameworks, nitrogen-containing heterocycles have been particularly common and a variety of derivatives of this latter type are available that provide coordination angles that range from 60° to 180°.[6a–6d]

We now report the synthesis of two new coordination frameworks incorporating iron(II) and cadmium(II) that are based on the new heterocyclic nitrogen derivative 1-(4-pyridyl)imino-2-(4-pyridyl)isoindoline (**L**). In comparison with the "classical" prototypical (linear) bis(pyridyl) ligand, 4,4′-bipyridyl,[6a–6d] the positions of the two pyridyl functions in **L** are more separated and the relative orientation of the coordination vectors is now angular. As occurs for other nonlinear bis(pyridyl) ligands such as 4,4′-dipyridyl sulfide,[7a,7b] a number of structural variations in the frameworks formed by **L** appeared possible. In part, the exploration of these possibilities provided a motivation for the investigation now reported.

[a] Centre for Heavy Metals Research, School of Chemistry, University of Sydney,
NSW 2006, Australia
E-mail: lindoy@chem.usyd.edu.au
[b] School of Physical and Chemical Sciences, Queensland University of Technology,
GPO Box 2434, Brisbane 4001, Australia
Supporting information for this article is available on the WWW under http://www.eurjic.org or from the author.

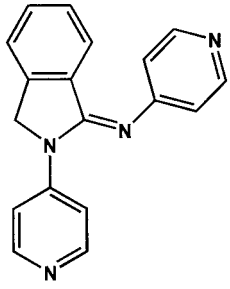

L

Results and Discussion

Ligand Synthesis

Isoindoline ring generation has been reported previously from the reaction of aniline with *o*-phthalaldehyde.[8] Using this methodology, *o*-phthalaldehyde was condensed with 4-aminopyridine in the present study to yield the isoindoline derivative **L**; the ESI mass spectral, ^1H NMR and microanalysis results confirmed the successful synthesis of this product.

Synthesis and Structures of the Frameworks

Treatment of **L** with cadmium(II) nitrate in ethanol produced colourless crystals of $[Cd\mathbf{L}(NO_3)_2(EtOH)]_n\cdot(1.4\,H_2O)_n$ that were stable in air at room temperature and proved suitable for an X-ray diffraction study. An ORTEP[9] representation of the asymmetric unit, plus a diagram illustrating the cadmium(II) coordination geometry, are presented in Figure 1. Pertinent geometric details are listed in Table 1.

The isoindoline derivative **L** bridges cadmium(II) centres creating a 1D chain-like coordination polymer (see a and b

  DOI: 10.1002/ejic.200500108

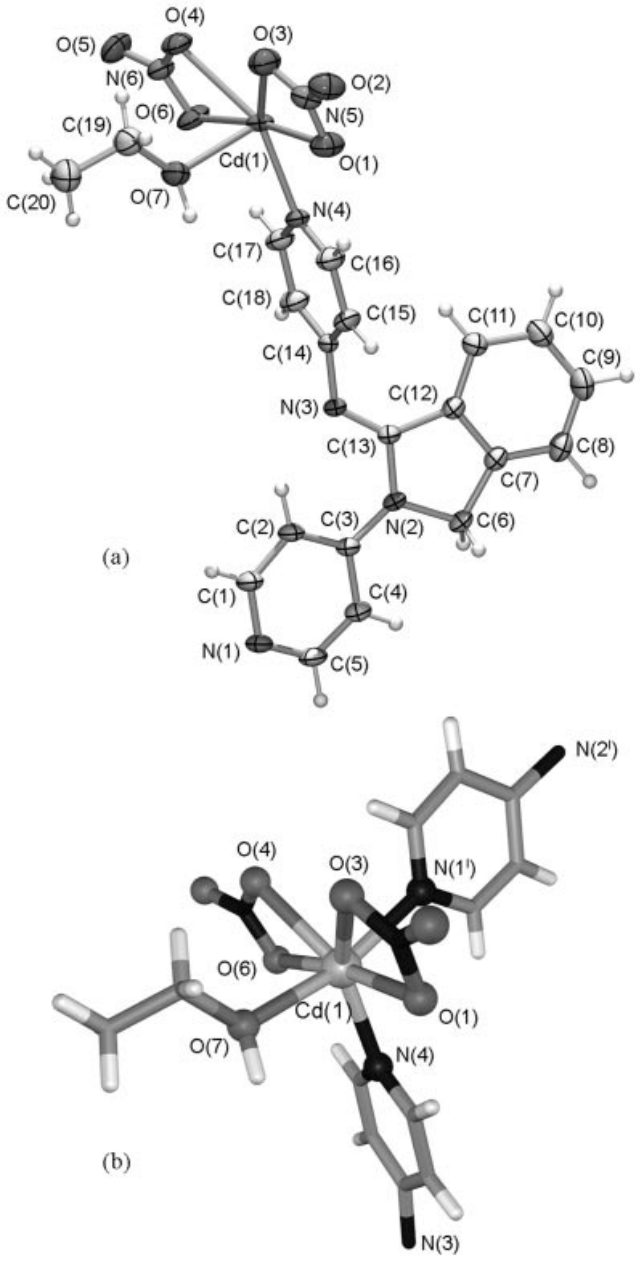

Figure 1. (a) An ORTEP representation of the asymmetric unit for the structure of $[Cd\mathbf{L}(NO_3)_2(EtOH)]_n\cdot(1.4\,H_2O)_n$ (50% ellipsoid probability, water solvate not shown). (b) Illustration of the approximate pentagonal bipyramidal cadmium(II) coordination geometry. The isoindoline ligands that coordinate via N(4) and N(1^I) have been truncated at N(3) and N(2^I) respectively. Symmetry code; ^{I} x, y, z + 1.

in Figure 2) with a repeating $[Cd\mathbf{L}(EtOH)(NO_3)_2]$ fragment that propagates parallel to the crystallographic c axis. The cadmium(II) ions are seven coordinate with approximate pentagonal bipyramidal stereochemistry. The pyridyl nitrogen atom N(4) binds within the pentagonal plane along with two nitrate anions (both bidentate). One pyramidal apex is occupied by an ethanol ligand while the other is occupied by the pyridyl nitrogen N(1) from an adjacent ligand in the chain. The individual chains propagate in a zigzag pattern reflecting the ca. 120° angle between the N donor atoms of the pyridyl groups which, in turn, is countered by a combination of the N(1^I)–Cd–N(4) coordination angle (104°) combined with a conformational contribution from the ligand (ca. 16°).

Table 1. Selected geometry details; bond lengths [Å] and angles [°] for $[Cd\mathbf{L}(NO_3)_2(EtOH)]_n\cdot(1.4\,H_2O)_n$.

Cd(1)–N(1^I)	2.283(2)	Cd(1)–O(4)	2.430(2)
Cd(1)–N(4)	2.279(2)	Cd(1)–O(6)	2.402(2)
Cd(1)–O(1)	2.476(2)	Cd(1)–O(7)	2.314(2)
Cd(1)–O(3)	2.462(2)		
		N(4)–Cd(1)–O(7)	90.62(8)
N(1^I)–Cd(1)–N(4)	104.76(8)	O(1)–Cd(1)–O(3)	51.85(8)
N(1^I)–Cd(1)–O(1)	89.49(9)	O(1)–Cd(1)–O(4)	133.18(8)
N(1^I)–Cd(1)–O(3)	83.75(9)	O(1)–Cd(1)–O(6)	171.61(8)
N(1^I)–Cd(1)–O(4)	88.11(8)	O(1)–Cd(1)–O(7)	88.01(9)
N(1^I)–Cd(1)–O(6)	96.68(9)	O(3)–Cd(1)–O(4)	81.44(8)
N(1^I)–Cd(1)–O(7)	164.19(9)	O(3)–Cd(1)–O(6)	134.36(8)
N(4)–Cd(1)–O(1)	85.71(8)	O(3)–Cd(1)–O(7)	82.44(9)
N(4)–Cd(1)–O(3)	137.02(9)	O(4)–Cd(1)–O(6)	53.06(7)
N(4)–Cd(1)–O(4)	139.73(8)	O(4)–Cd(1)–O(7)	82.27(8)
N(4)–Cd(1)–O(6)	87.22(8)	O(6)–Cd(1)–O(7)	87.56(9)

^{I} x, y, z + 1

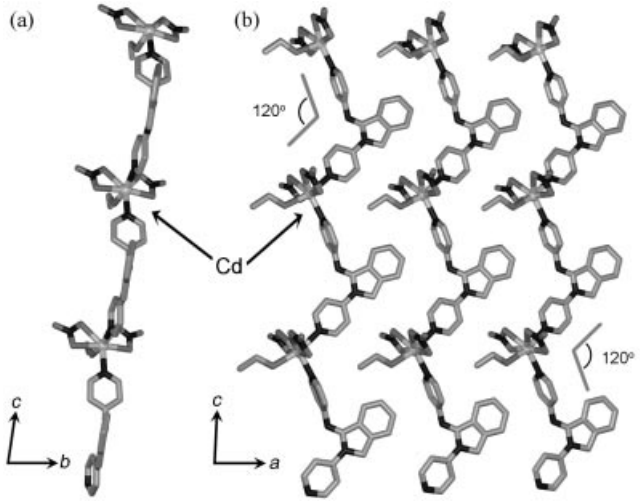

Figure 2. (a) The 1D coordinate polymer chains in $[Cd\mathbf{L}(NO_3)_2(EtOH)]_n\cdot(1.4\,H_2O)_n$ propagate parallel to the c axis. (b) Adjacent chains are aligned in sheets parallel to the ac plane. The individual chains display a 120° zigzag motif that derives from the angle between the N-donor directions countered predominantly by the coordination geometry at the cadmium(II) centre.

Adjacent 1D chains are co-aligned to produce sheets parallel to the ac plane.

These sheets are paired by a combination of offset face-to-face (π···π) interactions between the isoindoline components and edge-to-face (CH···π) interactions between the pyridyl groups of ligands in adjacent sheets (see Figure 1S in the Supporting Information). The isoindoline components involved in the offset face-to-face interactions are arranged with crystallographic inversion symmetry so that the five-membered rings overlap the six-membered rings with a mean plane-plane distance of 3.60 Å. The edge-to-face interactions between pyridyl groups occur with a CH_{edge}–

Py_{plane} distance of ca. 2.91 Å. Both distances fall in the normal range for each interaction type.[10,11]

The crystal lattice is depicted in Figure 3. Pairs of sheets stack parallel to the *ac* plane to produce channels, occupied by disordered water molecules, that run parallel to the *a* axis (see Figure 2S, Supporting Information). The solvent accessible volume in these channels constitutes approximately 21% of the total crystal volume.

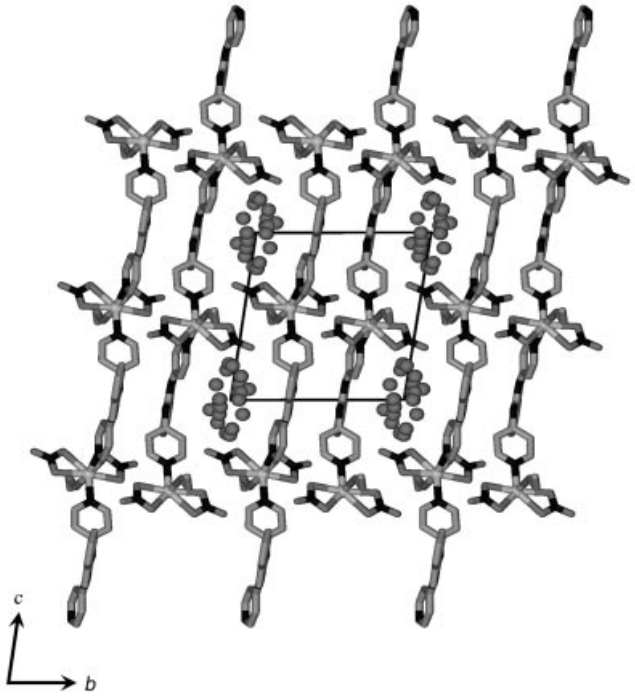

Figure 3. The crystal lattice viewed along the *a* axis. Disordered water molecules occupy channels between the paired sheets of polymeric complexes.

On reaction with iron(II) thiocyanate, **L** yielded the porous framework, $[Fe\mathbf{L}_2(NCS)_2]_n \cdot \{(2\,CHClCCl_2) \cdot (1.4\,MeOH) \cdot (2.9\,H_2O)\}_n$, in which the iron(II) ions subtend with two-dimensional polymeric connectivity. An ORTEP representation of the asymmetric unit and an illustration of the coordination geometry of the iron(II) centre are provided in Figure 4. Pertinent geometry details are listed in Table 2. The iron(II) centre has approximate octahedral stereochemistry with four pyridyl nitrogen atoms (from four separate ligand molecules) coordinated in equatorial positions and thiocyanato ligands *N*-coordinated in axial positions.

The above coordination connectivity results in infinite 2D rhombic grids (Figure 5) that propagate parallel to the *ab* plane; the grids have diagonal dimensions of 13 Å and 22 Å. The rhombic grids stack in the third dimension (along the *c* axis) with contiguous grids alternately offset. The observation of stacked rhombic grids is in contrast to our previous observation of an interpenetrated network structure with *trans*-4,4′-azopyridine (L′) of type $Fe_2(L')_4(NCS)_4 \cdot$(guest) which displays guest-dependent spin crossover.[2]

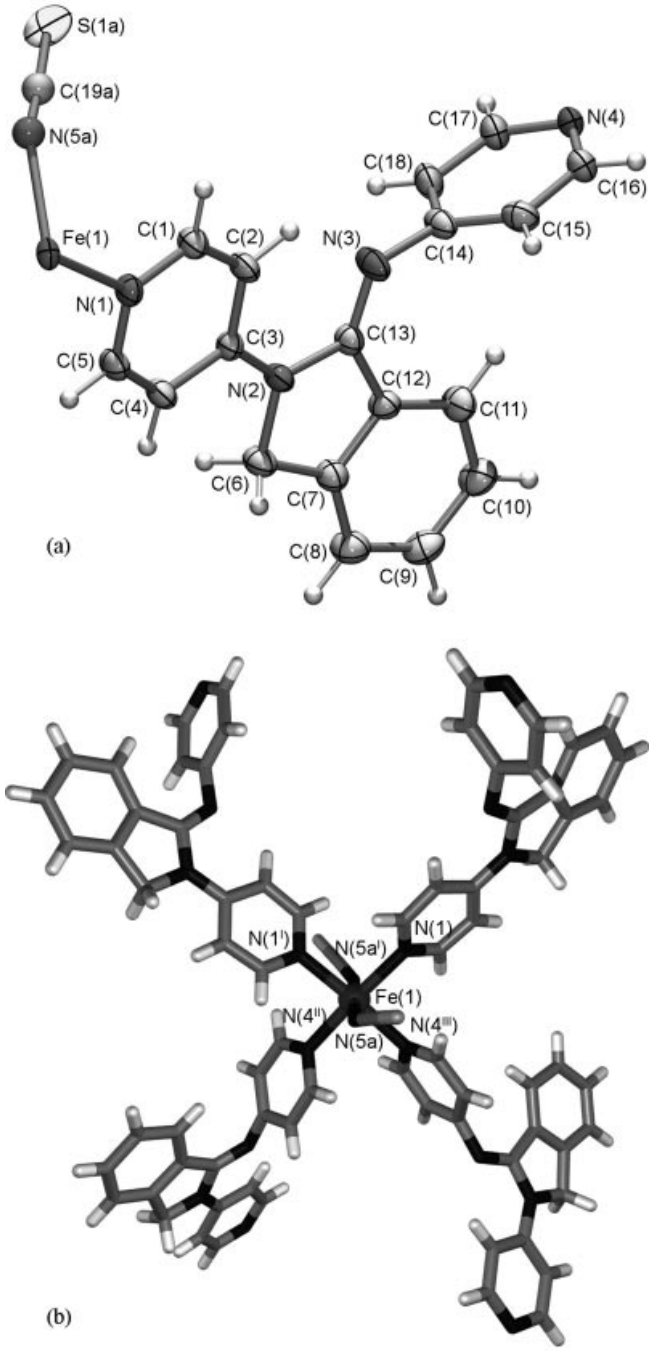

Figure 4. (a) An ORTEP representation of the asymmetric unit in $[Fe\mathbf{L}_2(NCS)_2]_n \cdot \{(2\,CHClCCl_2) \cdot (1.4\,MeOH) \cdot (2.9\,H_2O)\}_n$ (50% probability ellipsoids, solvent and the lower occupancy position of the disordered thiocyanato ligand omitted). (b) The coordination geometry at the iron(II) centre is approximately octahedral. Each iron(II) atom is equatorially bound to four pyridyl nitrogen atoms of four independent isoindoline ligands. Axial positions are occupied by thiocyanato groups.

A SQUID magnetism study of a vacuum-dried sample of the present framework was undertaken from 5 K to 300 K and showed a constant magnetic moment value corresponding to high spin iron(II) of μ_{eff}/μ_B = 5.2 between 80 and 300 K with no evidence for spin-crossover behaviour (zero-field splitting, rather than spin crossover, caused an

Table 2. Selected geometry details (bond lengths in Å, angles in °) for $[FeL_2(NCS)_2]_n \cdot \{(2\,CHClCCl_2) \cdot (1.4\,MeOH) \cdot (2.9\,H_2O)\}_n$.

Fe(1)–N(1)	2.202(4)	Fe(1)–N(5a)	2.137(5)
Fe(1)–N(4^{II})	2.223(4)		
		N(1)–Fe(1)–N(4^{III})	88.83(15)
N(1)–Fe(1)–N(5a)	88.8(3)	N(1^{I})–Fe(1)–N(4^{II})	88.83(15)
N(1)–Fe(1)–N($5a^{I}$)	91.0(2)	N(1^{I})–Fe(1)–N(4^{III})	176.80(15)
N(5a)–Fe(1)–N($5a^{I}$)	179.7(5)	N(4^{II})–Fe(1)–N(4^{III})	88.1(2)
N(1^{I})–Fe(1)–N($5a^{I}$)	88.8(3)	N(4^{II})–Fe(1)–N(5a)	91.8(3)
N(1^{I})–Fe(1)–N(5a)	91.0(2)	N(4^{III})–Fe(1)–N($5a^{I}$)	91.8(3)
N(1)–Fe(1)–N(1^{I})	94.3(2)	N(4^{II})–Fe(1)–N($5a^{I}$)	88.4(2)
N(1)–Fe(1)–N(4^{II})	176.80(15)	N(4^{III})–Fe(1)–N(5a)	88.4(2)

^{I} $-x + 1, y, -z + 3/2$; ^{II} $x - 1/2, y - 1/2, -z + 3/2$; ^{III} $-x + 3/2, y - ½, z$

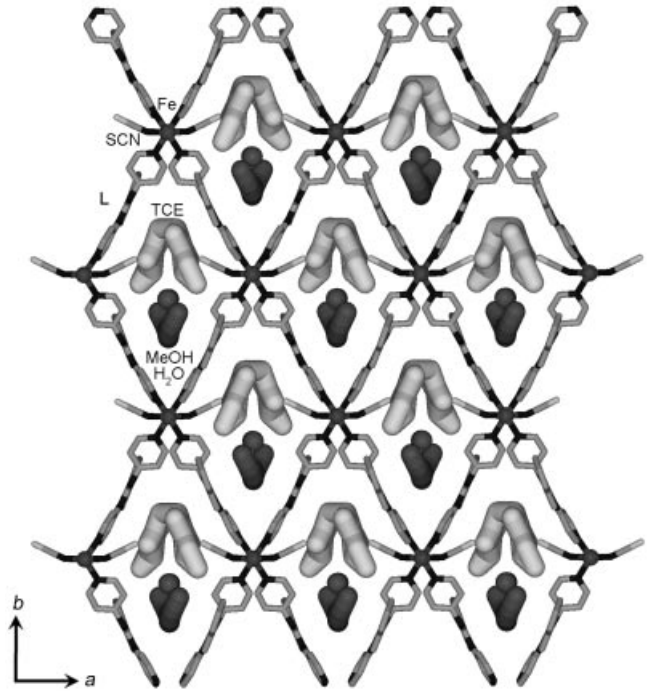

Figure 5. The difunctional isoindoline ligands connect iron atoms to produce rhombic grids. A section of each pore in the grid is occupied by disordered trichloroethylene and the remaining space in the pore is occupied by disordered water and methanol.

abrupt downturn in the effective magnetic moment below 50 K).

The pores in the present grid are solvated with a combination of water, methanol and trichloroethylene molecules. The polar water and methanol molecules are positioned on one side of each pore while the hydrophobic trichloroethylene molecules are positioned on the other. The overlap of the grids produces cavities occupied by trichloroethylene and continuous channels occupied by the water and methanol (this is illustrated in Figure 3S, Supporting Information). The solvent accessible regions in this framework constitute 42% of the total crystal volume and it is noted that solvent is rapidly lost from this product in air at room temperature with loss of crystallinity. Presumably the extensive solvation within the structure in this case provides an alternative to the formation of an interpenetrated arrangement that might otherwise serve to reduce the void volume.

Conclusions

Two new infinite molecular systems, one containing cadmium(II) and another containing iron(II), based on the nonlinear bis(pyridyl) ligand derivative **L** have been synthesised. The cadmium(II) framework is comprised of coaligned 1D coordinate polymer chains while the iron(II) framework consists of rhombic grids with 2D polymeric connectivity. Both crystal lattices are porous; the solvent accessible channels in the cadmium(II) framework constitute 21% of the crystal while those in the iron(II) framework constitute 42%.

Experimental Section

Reagents and Instrumentation: All reagents used for synthesis were obtained commercially and used without further purification. NMR spectra were recorded at 300 K on a Bruker DX300 Spectrometer. Low resolution electrospray mass spectra (ESI-MS) were obtained with a Finnigan LCQ-8 spectrometer. FTIR (DRIFTS) were collected with a Bio-Rad FTS-7 spectrometer. Magnetic susceptibility data were obtained using a Quantum Design MPMS SQUID magnetometer under an applied field of 1 T. The sample was first dispersed in petroleum jelly to prevent it from losing solvent. Diamagnetic corrections for the sample and sample holder were applied using Pascal constants. The magnetic susceptibility was measured from 5 K to 300 K. The final plot was obtained as μ_{eff}/μ_B value (where μ_{eff} is effective magnetic moment that equals to $(\chi_M T)^{1/2}$ and μ_B is Bohr magneton) as a function of temperature (K).

1-(4-Pyridyl)imino-2-(4-pyridyl)isoindoline Dihydrate (L·2H$_2$O): A mixture of *o*-phthalaldehyde (1.0 g, 0.007 mol), 4-aminopyridine (1.4 g, 0.014 mol), and glacial acetic acid (0.5 mL) in xylene (30 mL) was heated under reflux for 5 h to yield a yellow solution. Water was removed from the two-phase reaction using a Dean–Stark apparatus until the initial (two-phase) solution was homogeneous. The solution was then filtered and cooled in a refrigerator. The crude yellow product that precipitated was recrystallised from toluene to give a yellow microcrystalline solid of **L** as its dihydrate. Yield 1.5 g; 75%. $C_{18}H_{18}N_4O_2$ (322.4): calcd. C 67.07, H 5.63, N 17.38; found C 67.39, H 5.23, N 17.16. ^{1}H NMR (300 MHz, $CDCl_3$, 25 °C): δ = 8.54 (t, 5 H), 7.9 (dd, J = 1.65, 1.53 Hz, 2 H), 7.5 (m, 2 H), 7.16 (m, 1 H), 6.93 (m, 2 H), 4.97 (s, 2 H, CH_2) ppm. Mass Spectrum (ESI-MS): Found 287.3 m/z, $[M + H]^+$ requires 287.13 m/z.

[CdL(NO$_3$)$_2$]$_n$·(0.5H$_2$O)$_n$: Ligand **L** (0.02 g) was dissolved in ethanol (1 mL) and the solution placed in one side of a H-shaped glass cell. In the other side was placed a solution of cadmium(II) nitrate tetrahydrate (0.02 g) in ethanol (1 mL). The tube was then slowly filled with ethanol so that minimal mixing of the solution took place. A small quantity of colourless crystals (yield ca. 10%) with formula $[CdL(NO_3)_2(EtOH)]_n \cdot (1.4\,H_2O)_n$ suitable for X-ray analysis formed over a period of two weeks. The crystals were isolated and appeared stable in air over several days. They were dried under vacuum over P_2O_5 before microanalysis. The ethanol ligand and 0.9 water molecules per cadmium(II) were lost from the sample during

drying. $C_{18}H_{16}CdN_6O_{6.5}$ (532.8): calcd. C 40.58, H 3.03, N 15.77; found C 40.25, H 2.46, N 15.38.

$[FeL_2(NCS)_2]_n\cdot(H_2O)_n$: Iron(II) thiocyanate (0.08 mmol) in a mixture of trichloroethylene/methanol (2:1) 10 mL) was added to a solution of **L** (0.07 mmol) in the same solvent mixture (10 mL). The resulting red-orange solution slowly changed colour to red and after several days and orange crystals with formula $[Fe\mathbf{L}_2(NCS)_2]_n\cdot\{(2\,CHClCCl_2)\cdot(1.4\,MeOH)\cdot(2.9\,H_2O)\}_n$ suitable for X-ray structure determination formed. The crystals (0.03 g, 78%) were isolated and dried under vacuum over P_2O_5, resulting in loss of all solvate except one water molecule (per iron(II)), prior to microanalysis. $C_{38}H_{30}FeN_{10}OS_2$ (762.7): calcd. C 59.84, H 3.96, N 18.36; found C 59.19, H 3.56, N 18.13. A second preparation of this complex was carried out using a dichloromethane/methanol (2:1) solvent mixture. The unit cell constants for a crystal from this batch were determined to be the same as those in crystals obtained from the trichloroethylene/methanol crystallisation experiment.

X-ray Crystallographic Study: Data were collected at 150(2) K with ω scans to approximately 56° 2θ using a Bruker SMART 1000 diffractometer employing graphite-monochromated Mo-$K\alpha$ radiation generated from a sealed tube (0.71073 Å). Data integration and reduction were undertaken with SAINT and XPREP[12] and subsequent computations were carried out using the WinGX-32 graphical user interface.[13a,13b] Multi-scan empirical absorption corrections were applied to the data using the program SADABS.[14] The structures were solved by direct methods using SIR97[15] then refined and extended with SHELXL-97.[16]

In general, ordered non-hydrogen atoms were refined anisotropically. Partial occupancy non-hydrogen atoms were refined isotropically. Carbon-bound hydrogen atoms were included in idealised positions and refined using a riding model. Refinement residuals are defined as $R_1 = \Sigma||F_o| - |F_c||/\Sigma|F_o|$ for $F_o > 2\sigma(F_o)$ and $wR_2 = \{\Sigma[w(F_o^2 - F_c^2)^2]/\Sigma[w(F_c^2)^2]\}^{1/2}$ where $w = 1/[\sigma^2(F_o^2) + (\mathbf{A}P)^2 + \mathbf{B}P]$, $P = (F_o^2 + 2F_c^2)/3$ and A and B are listed with the crystal data for each structure.

$[CdL(NO_3)_2(EtOH)]_n\cdot(1.4\,H_2O)_n$: Formula $C_{20}H_{20}CdN_6O_7\cdot(H_2O)_{1.4}$, M = 594.04, triclinic, space group $P\bar{1}$ (no. 2), a = 9.105(2) Å, b = 12.106(3) Å, c = 12.494(3) Å, α = 80.891(4)°, β = 86.483(3)°, γ = 80.048(4), V = 1338.5(5) Å^3, D_c = 1.474 g cm^{-3}, Z = 2, crystal size 0.265 × 0.184 × 0.162 mm, colour colourless, habit multi-faced, temperature 150(2) K, λ(Mo-K_α) = 0.71073, μ(Mo-K_α) 0.869 mm^{-1}, T(empirical)$_{min,max}$ = 0.712, 0.869, $2\theta_{max}$ = 56.6, hkl range –11 to 12, –15 to 15, –16 to 16, N = 13064, N_{ind} = 6101 (R_{merge} = 0.0214), $N_{obsd.}$ = 5490 [$I > 2\sigma(I)$], N_{var} = 341, residuals $R_1(F, 2\sigma)$ = 0.0380, $wR_2(F^2$, all) = 0.1131, A = 0.0705, B = 0.7933, GoF(all) = 1.117, $\Delta\rho_{min,max}$ = –0.674, 1.014 e$^-$Å^{-3}.

Individual details: The water solvate is diffuse and was modelled with oxygen atoms in ten different positions, O(1W)–O(10W), with site occupancies between 0.1 and 0.2 to a total occupancy of 1.4 water molecules per asymmetric unit. H(7OE) attached to the ethanol oxygen atom O(7), was located in the difference map and refined (isotropically) with a 1.0 Å O–H bond length restraint.

$[FeL_2(NCS)_2]_n\cdot\{(2\,CHClCCl_2)\cdot(1.4\,MeOH)\cdot(2.9\,H_2O)\}_n$: Formula $C_{38}H_{28}FeN_{10}S_2\cdot(C_2HCl_3)_2\cdot(CH_4O)_{1.4}\cdot(H_2O)_{2.9}$, M = 1104.54, orthorhombic, space group *Pbcn* (no. 60), a = 13.045(3) Å, b = 22.026(5) Å, c = 17.824(4) Å, V = 5121(2) Å^3, D_c = 1.433 g cm^{-3}, Z = 4, crystal size 0.216 × 0.143 × 0.110 mm, colour orange, habit irregular, temperature 150(2) K, λ(Mo-K_α) = 0.71073, μ(Mo-K_α) 0.741 mm^{-1}, T(empirical)$_{min,max}$ = 0.810, 0.920, $2\theta_{max}$ = 56.6, hkl range –17 to 17, –29 to 29, –23 to 23, N = 20669, N_{ind} = 6279 (R_{merge} = 0.0571), $N_{obsd.}$ = 4288 [$I > 2\sigma(I)$], N_{var} = 270, residuals $R_1(F, 2\sigma)$ = 0.1017, $wR_2(F^2$, all) = 0.3240, A = 0.1762, B = 25.8136, GoF(all) = 1.038, $\Delta\rho_{min,max}$ = –1.781, 1.478 e$^-$Å^{-3}.

Individual details: The asymmetric unit comprises half of one iron(II) atom (Fe on twofold site), one ligand **L** and one thiocyanato ligand. The thiocyanato ligand displays minor disorder and was modelled in two positions, N(5a)–C(19a)–S(1a) and N(5b)–C(19b)–S(1b), with site occupancies of 0.8 and 0.2 respectively. The asymmetric unit also contained regions of smeared electron density associated with diffuse solvent molecules. Using three possible solvents (trichloroethylene, methanol and water), attempts were made to model this diffuse solvent. The most plausible model comprises 1 trichloroethylene (three positions with occupancies 0.5, 0.3 and 0.2), 0.7 methanol (two positions with occupancies 0.4 and 0.3) and 1.45 water (five positions with occupancies 0.4, 0.3, 0.25, 0.25 and 0.25) molecules per asymmetric unit. For comparative purposes, the electron density associated with the disordered solvent was removed from the intensity data using the SQUEEZE function of PLATON.[17a,17b] The cell void volume (in the absence of modelled solvent) was determined to be *c*. 2160 Å^3 which constitutes 42% of the total unit cell volume. The approximate electron count (determined by PLATON) associated with the cell void is 816 electrons (i.e. 102 electrons per asymmetric unit). This is reasonably consistent with the total count of electrons used in the disordered solvent model (87 electrons per asymmetric unit). The residuals obtained upon structure refinement after the application of SQUEEZE [$R_1(F,2\sigma)$ = 0.0463, $wR_2(F^2$,all) = 0.1240] were very acceptable and considerably lower than the residuals obtained upon refinement of the solvated model [$R_1(F,2\sigma)$ = 0.1017, $wR_2(F^2$,all) = 0.3240]. It appears from the SQUEEZE analysis that the high residuals in the reported structure are artefacts of (unavoidable) inadequacies in the solvent model. All disordered components (except water) were refined as rigid groups.

CCDC-258885 and -258886 contain the supplementary crystallographic data for this paper. These data can be obtained free of charge from The Cambridge Crystallographic Data Centre via www.ccdc.cam.ac.uk/data_requst/cif.

Supporting Information (see also footnote on the first page of this article): Figures showing how the sheets in $[Cd\mathbf{L}(NO_3)_2(EtOH)]_n\cdot(1.4\,H_2O)_n$ are paired through offset face-to-face π interactions and edge-to-face π interactions; the surface contours of the solvent accessible channels in $[Cd\mathbf{L}(NO_3)_2(EtOH)]_n\cdot(1.4\,H_2O)_n$ and a view of the $[Fe\mathbf{L}_2(NCS)_2]_n\cdot\{(2\,CHClCCl_2)\cdot(1.4\,MeOH)\cdot(2.9\,H_2O)\}_n$ lattice parallel to the *c* axis. In the latter case the grids stack along the *c* axis with adjacent grids offset from one another. The effect of this is to enclose the trichloroethylene in noncontinuous cavities while the water and methanol molecules occupy the continuous channels in the porous framework.

Acknowledgments

We thank the Australian Research Council for support and Prof. K. S. Murray and Dr. B. Moubaraki of Monash University for undertaking the variable temperature magnetic measurements.

[1] a) M. Fujita, Y. J. Kwon, S. Washizu, K. Ogura, *J. Am. Chem. Soc.* **1994**, *116*, 1151; b) J. Lu, T. Paliwala, S. C. Lim, C. Yu, T. Niu, A. J. Jacobson, *Inorg. Chem.* **1997**, *36*, 923; c) R.-D. Schnebeck, L. Randaccio, E. Zangrado, B. Lippert, *Angew. Chem. Int. Ed. Engl.* **1998**, *37*, 119; d) K. N. Power, T. L. Hennigar, M. J. Zaworotko, *New J. Chem.* **1998**, *22*, 177; e) M. Kondo, M. Shimamura, S. Noro, S. Minakoshi, A. Asami, K. Seiki, S. Kitagawa, *Chem. Mater.* **2000**, *12*, 1288; f) Y. Zhang,

L. Jianmin, M. Nishiura, T. Imamoto, *J. Mol. Struct.* **2000**, *519*, 219; g) A. N. Khlobystov, A. J. Blake, N. R. Champness, D. A. Lemenovskii, A. G. Majouga, N. V. Zyk, M. Schröder, *Coord. Chem. Rev.* **2001**, *222*, 155; h) S. A. Barnett, N. R. Champness, *Coord. Chem. Rev.* **2003**, *246*, 145; i) S. L. James, *Chem. Soc. Rev.* **2003**, *32*, 276; j) G. S. Papaefstathiou, L. R. MacGillivray, *Coord. Chem. Rev.* **2003**, *246*, 169; k) M. J. Rosseinsky, *Microporous Mesoporous Mater.* **2004**, *73*, 15.

[2] G. J. Halder, C. J. Kepert, B. Moubaraki, K. S. Murray, J. D. Cashion, *Science* **2002**, *298*, 1762.

[3] a) H. J. Choi, T. S. Lee, M. P. Suh, *Angew. Chem. Int. Ed.* **1999**, *38*, 1405; b) C. J. Kepert, M. J. Rosseinsky, *Chem. Commun.* **1999**, 375; c) K. S. Min, M. P. Suh, *J. Am. Chem. Soc.* **2000**, *122*, 6834; d) E. J. Cussen, J. B. Claridge, M. J. Rosseinsky, C. J. Kepert, *J. Am. Chem. Soc.* **2002**, *124*, 9574; e) C. Janiak, *Dalton Trans.* **2003**, 2781.

[4] a) M. Eddaoudi, J. Kim, N. Rosi, D. Vodak, J. Wachter, M. O'Keefe, O. M. Yaghi, *Science* **2002**, *295*, 469; b) N. L. Rosi, J. Eckert, M. Eddaoudi, D. T. Vodak, J. Kim, M. O'Keefe, O. M. Yaghi, *Science* **2004**, *300*, 1127.

[5] J. S. Seo, D. Whang, H. Lee, S. I. Jun, J. Oh, Y. J. Jeon, K. Kim, *Nature* **2000**, *404*, 982.

[6] a) P. J. Stang, B. Olenyuk, *Acc. Chem. Res.* **1997**, *30*, 502; b) S. Leininger, B. Olenyuk, P. J. Stang, *Chem. Rev.* **2000**, *100*, 853; c) J. A. R. Navarro, B. Lippert, *Coord. Chem. Rev.* **2001**, *222*, 219; d) S. R. Seidel, P. J. Stang, *Acc. Chem. Res.* **2002**, *35*, 972.

[7] a) C. S. Lai, E. R. T. Tiekink, *Cryst. Eng. Commun.* **2004**, *6*, 593; b) S. Muthu, Z. Ni, J. J.Vittal, *Inorg. Chim. Acta* **2005**, *358*, 595.

[8] S. Nan′ya, T. Tange, E. Maekawa, *J. Heterocycl. Chem.* **1985**, *22*, 449.

[9] ORTEP-3, L. J. Farrugia, *J. Appl. Crystallogr.* **1997**, *30*, 565.

[10] C. Janiak, *J. Chem. Soc. Dalton Trans.* **2000**, 3885.

[11] M. Nishio, M. Hirota, Y. Umezawa, The CH/pi interaction, Wiley-VCH, New York, **1998**.

[12] Bruker; SMART, SAINT and XPREP: Area detector control and data integration and reduction software, Bruker Analytical X-ray Instruments Inc., Madison, Wisconsin, USA, **19<95**.

[13] a) WinGX-32: System of programs for solving, refining and analysing single-crystal X-ray diffraction data for small molecules; b) L. J. Farrugia, *J. Appl. Crystallogr.* **1999**, *32*, 837.

[14] G. M. Sheldrick, SADABS: empirical absorption and correction software, University of Göttingen, Göttingen, Germany, **1999**.

[15] A. Altomare, M. C. Burla, M. Camalli, G. L. Cascarano, C. Giocavazzo, A. Guagliardi, A. G. C. Moliterni, G. Polidori, S. Spagna, *J. Appl. Crystallogr.* **1999**, *32*, 115.

[16] G. M. Sheldrick, SHELX-97: programs for crystal structure analysis, University of Göttingen, Göttingen, Germany, **1998**.

[17] a) A. L. Spek, *Acta Crystallogr. Sect. C* **1990**, *46*, 34; b) P. van der Sluis, A. L. Spek, *Acta Crystallogr.* **1990**, *46*, 194.

Received: February 03, 2005

